

PROBING THE NUCLEAR EQUATION OF STATE IN THE MULTI-MESSENGER ASTRONOMY ERA

Insights from Gravitational Waves

Polychronis S. Koliogiannis

Department of Physics, Faculty of Science, University of Zagreb, Bijenička cesta 32, 10000 Zagreb, Croatia
Department of Nuclear and Elementary Particle Physics, Faculty of Sciences, Aristotle University of Thessaloniki

August 5-7, 2024
Institute of Theoretical Physics, University of Warsaw
Warsaw, Poland

*Brainstorming workshop: Deciphering the equation of state using gravitational waves
from astrophysical sources*



Financira
Europska unija
NextGenerationEU



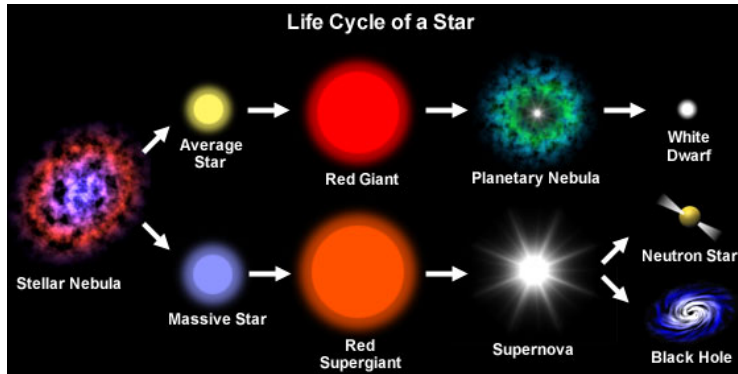
Table of Contents I

- 1 Stellar Remnants
- 2 EOS & Neutron stars
 - Cold equation of state
 - Hot equation of state
 - Momentum dependent interaction model
 - Cold neutron star matter
 - Thermodynamics of hot neutron star matter
 - Isothermal process
 - Leptons contribution
 - Equation of state
- 3 Isolated non-rotating and maximally-rotating Neutrons stars
 - Equation of state, adiabatic index and speed of sound
 - Thermal effects on non-rotating neutron stars and the threshold mass
 - Moment of inertia, kerr parameter and ratio T/W on rotating neutron stars
- 4 Hot rapidly rotating remnant
- 5 Last orbits of an inspiraling binary neutron star system
- 6 Microscopic properties of finite nuclei - GW events
- 7 Conclusions

Stellar Remnants

The endpoints of stellar evolution can take one of the three forms

- White Dwarf ($M \lesssim 8 M_{\odot}$)
- Neutron Star ($8 M_{\odot} \lesssim M \lesssim 20 M_{\odot}$)
- Black Hole ($M \gtrsim 20 M_{\odot}$)



Stellar Remnants

The endpoints of stellar evolution can take one of the three forms

- White Dwarf ($M \lesssim 8 M_{\odot}$)
- Neutron Star ($8 M_{\odot} \lesssim M \lesssim 20 M_{\odot}$)
- Black Hole ($M \gtrsim 20 M_{\odot}$)

Neutron Star

- Mass: $1.4\text{--}2.5 M_{\odot}$
- Eq. Radius: $10\text{--}15 km$
- Mean density: $4 \times 10^{14} gr/cm^3$
- Frequency: up to $2.2 kHz$



The highest masses of observable neutron stars are : $M_{\max} = 2.01 M_{\odot}$,

$M_{\max} = 2.14 M_{\odot}$, and $M_{\max} = 2.35 M_{\odot}$

The fastest observed rotating neutron star is at $716 Hz$

Stellar Remnants

Why we study Neutron Stars

- They are the most compact stars known to exist in the universe
- They have densities equal to that of the early universe
- Gravity is similar to that of a black hole
- They have the most extreme magnetic fields known in the universe (up to $10^{16}G$)
- They considered as extraordinary astronomical laboratories for the physics of nuclear matter
- They possibly appear phase transition in to other degrees of freedom (quarks, hyperons etc.)
- They provide a check for General Relativity
- They present a unique interplay among **astrophysics**, **gravitational physics** and **nuclear physics**

Cold equation of state

Neutron stars

- Long-live neutron stars
- Protons + Neutrons + Leptons
- Cold EOSs
- $T \ll 0.01$ MeV

Hot equation of state

Protoneutron stars

- Shortly after neutron stars born
- Trapped neutrinos
- Protons + Neutrons + Leptons

T (MeV)	Y_l	S (k_B)
0 - 50	0.01 - 0.4	0 - 10

Hot neutron stars

- Heat up by mass accretion due to a companion (Neutron stars merger)
- Protons + Neutrons + Leptons

T (MeV)	Y_l	S (k_B)
0 - 100	0.01 - 0.6	0 - 100

Momentum dependent interaction model

The energy of asymmetric nuclear matter is given by the relation

$$\mathcal{E}(n_n, n_p, T) = \mathcal{E}_{\text{kin}}^n(n_n, T) + \mathcal{E}_{\text{kin}}^p(n_p, T) + V_{\text{int}}(n_n, n_p, T), \quad (1)$$

- kinetic part: $\mathcal{E}_{\text{kin}}^n(n_n, T) + \mathcal{E}_{\text{kin}}^p(n_p, T)$
- interaction part: $V_{\text{int}}(n_n, n_p, T)$

Momentum dependent interaction model

- $\mathcal{E}_{\text{kin}}^n(n_n, T) + \mathcal{E}_{\text{kin}}^p(n_p, T)$

$$\mathcal{E}_{\text{kin}}^\tau(n_\tau, T) = 2 \int \frac{d^3k}{(2\pi)^3} \frac{\hbar^2 k^2}{2m} f_\tau(n_\tau, k, T), \quad (2)$$

where the Fermi-Dirac distribution is

$$f_\tau(n_\tau, k, T) = \left[1 + \exp \left(\frac{e_\tau(n_\tau, k, T) - \mu_\tau(n_\tau, T)}{T} \right) \right]^{-1}, \quad (3)$$

with nucleon density and single particle energy evaluated through

$$n_\tau = 2 \int \frac{d^3k}{(2\pi)^3} f_\tau(n_\tau, k, T), \quad \text{and} \quad e_\tau(n_\tau, k, T) = \frac{\hbar^2 k^2}{2m} + U_\tau(n_\tau, k, T). \quad (4)$$

Momentum dependent interaction model

- $V_{\text{int}}(n_n, n_p, T)$

$$V_{\text{int}}(n_n, n_p, T) = V_A + V_B + V_C, \quad (5)$$

where

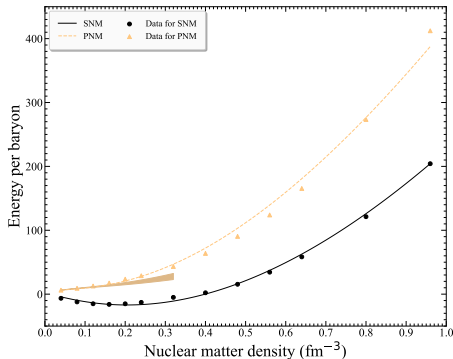
$$V_A = \frac{1}{3} A n_s \left[\frac{3}{2} - \left(\frac{1}{2} + x_0 \right) I^2 \right] u^2, \quad (6)$$

$$V_B = \frac{\frac{2}{3} B n_s \left[\frac{3}{2} - \left(\frac{1}{2} + x_3 \right) I^2 \right] u^{\sigma+1}}{1 + \frac{2}{3} B' \left[\frac{3}{2} - \left(\frac{1}{2} + x_3 \right) I^2 \right] u^{\sigma-1}}, \quad (7)$$

$$V_C = u \sum_{i=1,2} \left[C_i \left(\mathcal{J}_n^i + \mathcal{J}_p^i \right) + I \frac{(C_i - 8Z_i)}{5} \left(\mathcal{J}_n^i - \mathcal{J}_p^i \right) \right], \quad (8)$$

- n_s denotes the saturation density and $u = n/n_s$
- $I = 1 - 2Y_p$ is the asymmetry parameter and Y_p is the proton fraction
- $[A, B, B', C_i]$ are the parameters for SNM, $[x_0, x_3, Z_i]$ are the parameters for ANM
- $\mathcal{J}_\tau^i = 2 \int \frac{d^3 k}{(2\pi)^3} g(k, \Lambda_i) f_\tau(n_\tau, k, T)$ with $g(k, \Lambda_i) = \left[1 + \left(\frac{k}{\Lambda_i} \right)^2 \right]^{-1}$

Momentum dependent interaction model



Properties of NM	MDI+APR1	Units
L_{sym}	77.696	MeV
Q_{sym}	223.061	MeV
K_{sym}	0.016	MeV
E_{sym}	31.071	MeV
Q_s	-25.687	MeV
K_s	220.671	MeV
m_τ^*/m_τ	0.822	

- MDI + data from Akmal *et al*¹
- 1 Cold EOS + nine hot EOSs based on various lepton fractions and entropies per baryon in the ranges [0.2, 0.4] and [1, 3] k_B , respectively.

¹ A. Akmal, V. R. Pandharipande, and D. G. Ravenhall, Phys. Rev. C **58**, 1804 (1998).

² M. Piarulli, I. Bombaci, D. Logoteta, A. Lovato, and R. B. Wiringa, Phys. Rev. C **101**, 045801 (2020).

Momentum dependent interaction model

Properties of NM	MDI+APR1	Experiment	Units
L_{sym}	77.696	40-70	MeV
Q_{sym}	223.061	-	MeV
K_{sym}	0.016	-100 ± 200	MeV
E_{sym}	31.071	30-35	MeV
Q_s	-25.687	-700 ± 500	MeV
K_s	220.671	230 ± 30	MeV
m_τ^*/m_τ	0.822	0.8 ± 0.1	

- reproduces with high accuracy the properties of SNM
- reproduces correctly the microscopic calculations of the Chiral model and the results of state-of-the-art calculations of Akmal *et al*¹
- predicts M_{max} at least higher than the observed ones

¹ A. Akmal, V. R. Pandharipande, and D. G. Ravenhall, Phys. Rev. C **58**, 1804 (1998).

² M. Piarulli, I. Bombaci, D. Logoteta, A. Lovato, and R. B. Wiringa, Phys. Rev. C **101**, 045801 (2020).

Cold neutron star matter

- Matter consists of protons, neutrons and electrons in chemical equilibrium

$$n \rightleftharpoons p + e^-, \quad \mu_n = \mu_p + \mu_e \quad (9)$$

- Proton fraction from β -equilibrium is

$$\mu_e = \mu_n - \mu_p = -\frac{\partial \mathcal{E}}{\partial Y_p} \Bigg|_n \Rightarrow \frac{\partial \mathcal{E}}{\partial Y_p} \Bigg|_n = -\hbar c (3\pi^2 Y_p n)^{1/3} \quad (10)$$

Total energy density

$$\mathcal{E}_t(n, Y_p) = \mathcal{E}_b(n, Y_p) + \sum_l \mathcal{E}_l(n, Y_p), \quad (11)$$

Total pressure

$$P_t(n, Y_p) = P_b(n, Y_p) + \sum_l P_l(n, Y_p), \quad (12)$$

where

$$P_b(n, T, Y_p) = n^2 \frac{\partial \mathcal{E}_b(n, Y_p)}{\partial n} \text{ and } P_e(n, Y_p) = \frac{\hbar c}{12\pi^2} (3\pi^2 Y_p n)^{4/3}. \quad (13)$$

Thermodynamics of hot neutron star matter

- Helmholtz free energy

$$F(n, T, I) = E(n, T, I) - TS(n, T, I), \quad (14)$$

- Entropy density

$$s_\tau(n, T, I) = -g \int \frac{d^3 k}{(2\pi)^3} [f_\tau \ln f_\tau + (1 - f_\tau) \ln(1 - f_\tau)], \quad (15)$$

- Pressure and chemical potentials

$$P = -\left. \frac{\partial E}{\partial V} \right|_{S, N_i} = n^2 \left. \frac{\partial (\mathcal{E}/n)}{\partial n} \right|_{S, N_i}, \quad (16)$$

$$\mu_i = \left. \frac{\partial E}{\partial N_i} \right|_{S, V, N_j \neq i} = \left. \frac{\partial \mathcal{E}}{\partial n_i} \right|_{S, V, n_j \neq i}. \quad (17)$$

Isothermal process

Pressure and chemical potentials are connected with the free energy as

$$P = -\frac{\partial F}{\partial V} \Bigg|_{T, N_i} = n^2 \frac{\partial (f/n)}{\partial n} \Bigg|_{T, N_i}, \quad \mu_i = \frac{\partial F}{\partial N_i} \Bigg|_{T, V, N_j \neq i} = \frac{\partial f}{\partial n_i} \Bigg|_{T, V, n_j \neq i}, \quad (18)$$

The entropy per particle is given through the relation

$$S(n, T) = -\frac{\partial (f/n)}{\partial T} \Bigg|_{V, N_i} = -\frac{\partial F}{\partial T} \Bigg|_n. \quad (19)$$

The chemical potentials take the form

$$\mu_n = F + u \frac{\partial F}{\partial u} \Bigg|_{Y_p, T} - Y_p \frac{\partial F}{\partial Y_p} \Bigg|_{n, T}, \quad \mu_p = \mu_n + \frac{\partial F}{\partial Y_p} \Bigg|_{n, T}, \quad \hat{\mu} = \mu_n - \mu_p = -\frac{\partial F}{\partial Y_p} \Bigg|_{n, T}. \quad (20)$$

Isothermal process

The free energy $F(n, T, I)$ and the internal energy $E(n, T, I)$ can be expressed by the following parabolic approximations

$$F(n, T, I) = F(n, T, I = 0) + I^2 F_{\text{sym}}(n, T), \quad (21a)$$

$$E(n, T, I) = E(n, T, I = 0) + I^2 E_{\text{sym}}(n, T), \quad (21b)$$

Isothermal process

The free energy $F(n, T, I)$ and the internal energy $E(n, T, I)$ can be expressed by the following parabolic approximations

$$F(n, T, I) = F(n, T, I = 0) + I^2 F_{\text{sym}}(n, T), \quad (21a)$$

$$E(n, T, I) = E(n, T, I = 0) + I^2 E_{\text{sym}}(n, T), \quad (21b)$$

The key quantity of Eq. (20) can be obtained by using Eq. (21a) as

$$\hat{\mu} = \mu_n - \mu_p = 4(1 - 2Y_p)F_{\text{sym}}(n, T). \quad (22)$$

Isothermal process

The free energy $F(n, T, I)$ and the internal energy $E(n, T, I)$ can be expressed by the following parabolic approximations

$$F(n, T, I) = F(n, T, I = 0) + I^2 F_{\text{sym}}(n, T), \quad (21a)$$

$$E(n, T, I) = E(n, T, I = 0) + I^2 E_{\text{sym}}(n, T), \quad (21b)$$

The key quantity of Eq. (20) can be obtained by using Eq. (21a) as

$$\hat{\mu} = \mu_n - \mu_p = 4(1 - 2Y_p)F_{\text{sym}}(n, T). \quad (22)$$

It is intuitive to assume, based mainly on Eqs. (21a) and (21b), that the entropy must also exhibit a quadratic dependence on asymmetry parameter I , that is according to the parabolic law

$$S(n, T, I) = S(n, T, I = 0) + I^2 S_{\text{sym}}(n, T), \quad (23)$$

In general: $Q_{\text{sym}} = Q(n, T, I = 1) - Q(n, T, I = 0)$, where $Q = F, E, S$

Leptons contribution

β decay and electron capture would take place simultaneously as

$$n \longrightarrow p + e^- + \bar{\nu}_e, \quad \text{and} \quad p + e^- \longrightarrow n + \nu_e. \quad (24)$$

Leptons contribution

β decay and electron capture would take place simultaneously as



► Isothermal process

- $n + p + e$
- $\mu_n = \mu_p + \mu_e$
- $Y_p = Y_p(n)$

► Isentropic process

- $n + p + e + \nu_e$
- $\mu_n + \mu_{\nu_e} = \mu_p + \mu_e$
- $Y_p = Y_e$ and $Y_l = Y_e + Y_{\nu_e}$

key relation

$$\hat{\mu} = \mu_n - \mu_p = 4(1 - 2Y_p)F_{\text{sym}}(n, T)$$

Leptons contribution

β decay and electron capture would take place simultaneously as



► Isothermal process

- $n + p + e$
- $\mu_n = \mu_p + \mu_e$
- $Y_p = Y_p(n)$

► Isentropic process

- $n + p + e + \nu_e$
- $\mu_n + \mu_{\nu_e} = \mu_p + \mu_e$
- $Y_p = Y_e$ and $Y_l = Y_e + Y_{\nu_e}$

key relation

$$\hat{\mu} = \mu_n - \mu_p = 4(1 - 2Y_p)F_{\text{sym}}(n, T)$$

- In isentropic case we consider that: $Y_p = 2/3Y_l + 0.05$ within 3% accuracy ³

³ T. Takatsuka, PThPh **95**, 901-912 (1996).

Leptons contribution

The energy density and pressure of leptons are calculated through the following formulas

$$\mathcal{E}_l(n_l, T) = \frac{2}{(2\pi)^3} \int \frac{d^3 k \sqrt{\hbar^2 k^2 c^2 + m_l^2 c^4}}{1 + \exp \left[\frac{\sqrt{\hbar^2 k^2 c^2 + m_l^2 c^4} - \mu_l}{T} \right]}, \quad (25)$$

$$P_l(n_l, T) = \frac{1}{3} \frac{2(\hbar c)^2}{(2\pi)^3} \int \frac{1}{\sqrt{\hbar^2 k^2 c^2 + m_l^2 c^4}} \times \frac{d^3 k \ k^2}{1 + \exp \left[\frac{\sqrt{\hbar^2 k^2 c^2 + m_l^2 c^4} - \mu_l}{T} \right]}. \quad (26)$$

Equation of state

Total energy density

$$\mathcal{E}_t(n, T, Y_p) = \mathcal{E}_b(n, T, Y_p) + \sum_l \mathcal{E}_l(n, T, Y_p), \quad (27)$$

where

$$\mathcal{E}_b(n, T, Y_p) = nF_{\text{PA}} + nTS_{\text{PA}}. \quad (28)$$

Total pressure

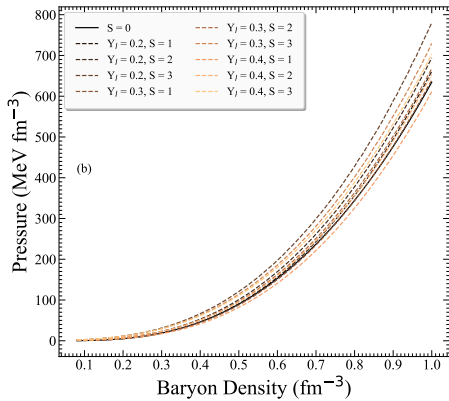
$$P_t(n, T, Y_p) = P_b(n, T, Y_p) + \sum_l P_l(n, T, Y_p), \quad (29)$$

where

$$P_b(n, T, Y_p) = n^2 \frac{\partial F_{\text{PA}}(n, T, Y_p)}{\partial n} \Bigg|_{T, n_i}. \quad (30)$$

Equation of state, adiabatic index and speed of sound

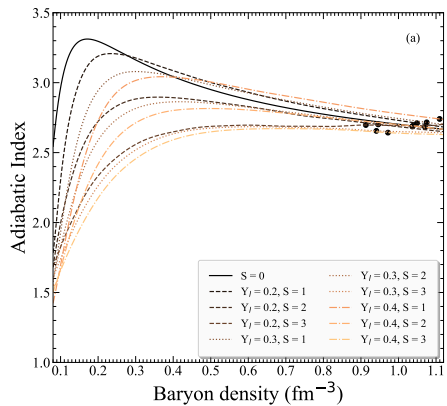
► Isentropic Equations of state



Equation of state, adiabatic index and speed of sound

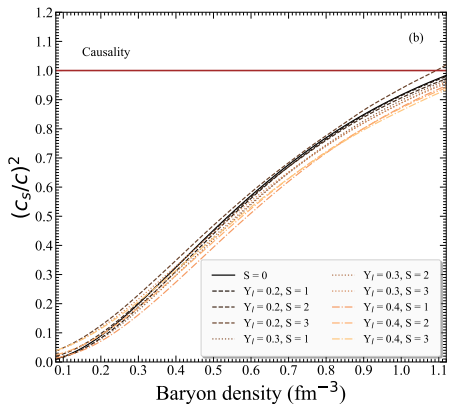
► Adiabatic index

$$\Gamma = \frac{n}{P} \frac{\partial P}{\partial n} \Big|_S \quad (31)$$



► Speed of sound

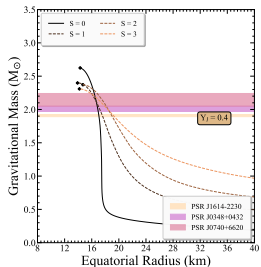
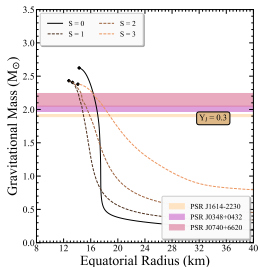
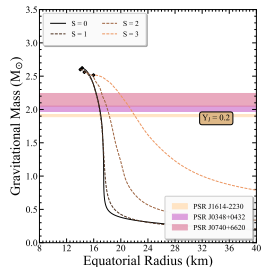
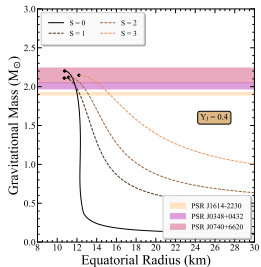
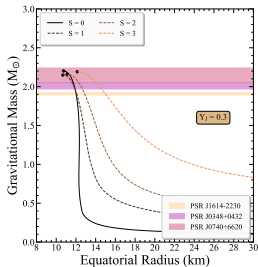
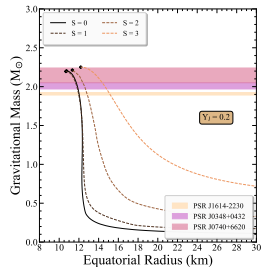
$$\frac{c_s}{c} = \sqrt{\frac{\partial P}{\partial E}} \Big|_S \quad (32)$$



Equation of state, adiabatic index and speed of sound

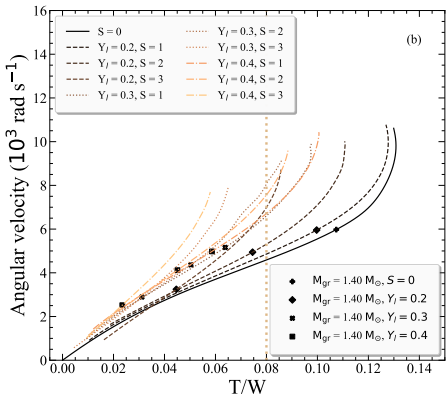
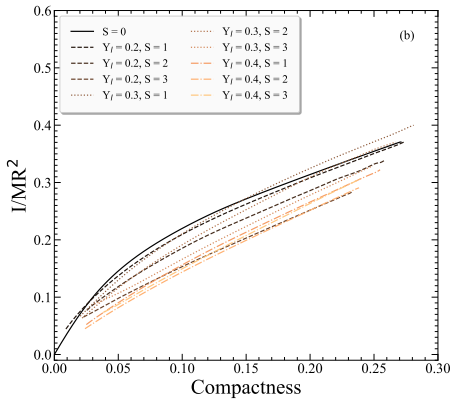
► Mass-radius diagram

Top panel: Nonrotating and Bottom panel: Maximally rotating



Moment of inertia, kerr parameter and ratio T/W on rotating neutron stars

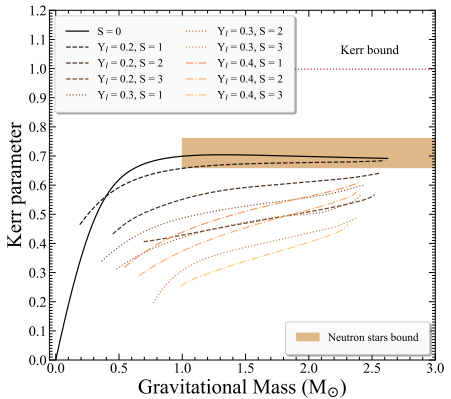
- The increase of temperature/entropy per baryon, except for some specific cases ($Y_l = 0.2, 0.3$ and $S = 1$), leads to lesser compact objects than the cold EOS
- For sufficiently compact neutron stars the non-axisymmetric instability will set in before the mass-shedding limit is reached



Moment of inertia, kerr parameter and ratio T/W on rotating neutron stars

- $\mathcal{K} \equiv cJ/(GM^2)$
- $\mathcal{K}_k \simeq 1.34\sqrt{\beta_{\max}}$ ⁷
- $0.24 \leq \beta_{\max} \leq 0.32 \Rightarrow 0.66 \leq \mathcal{K}_k \leq 0.76$

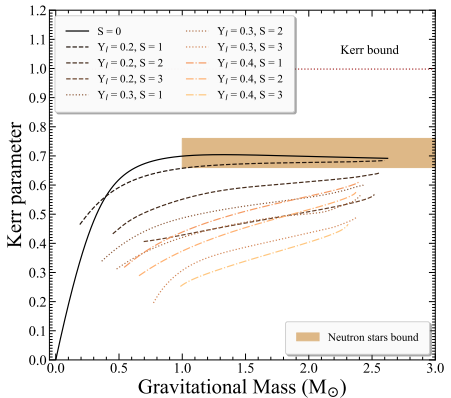
$$\mathcal{K}_{\text{B.H.}} \approx 0.998$$
8



⁷ P.S. Koliogiannis and Ch.C. Moustakidis, Phys. Rev. C **101**, 015805 (2020).

⁸ K.S. Thorne, ApJ **191**, 507-520 (1974).

Moment of inertia, kerr parameter and ratio T/W on rotating neutron stars



- $\mathcal{K}_{N.S.}$ and $\mathcal{K}_{B.H.}$ cannot be exceeded as the temperature in neutron stars increasing
- The gravitational collapse of a hot, uniformly rotating neutron star, cannot lead to a maximally rotating Kerr black hole

Hot rapidly rotating remnant

- Hot, rapidly rotating remnant: at least $S = 1$ and $Y_l = 0.2$
- $\beta_{\text{rem}}^{\text{ad}} \leq 0.27$
- $\mathcal{K}_{\text{rem}}^{\text{ad}} \leq 0.68$
- $(T/W)_{\text{rem}}^{\text{ad}} \leq 0.127$

Hot rapidly rotating remnant

- Hot, rapidly rotating remnant: at least $S = 1$ and $Y_l = 0.2$
- $\beta_{\text{rem}}^{\text{ad}} \leq 0.27$
- $\mathcal{K}_{\text{rem}}^{\text{ad}} \leq 0.68$
- $(T/W)_{\text{rem}}^{\text{ad}} \leq 0.127$

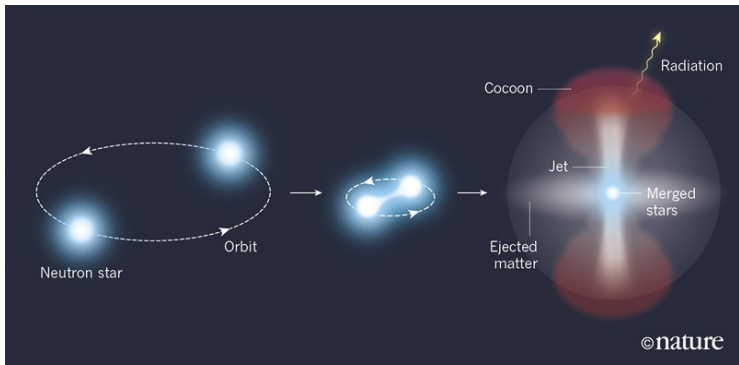
Isentropic EOS - Presented case

- object comparable to the one of cold EOS
- unstable toward the dynamical instabilities

Isentropic EOS - Rest cases

- lesser compact star than the cold EOS, with lower values of maximum gravitational mass and frequency
- more stable toward the dynamical instabilities by increasing S

Last orbits of an inspiraling binary neutron star system



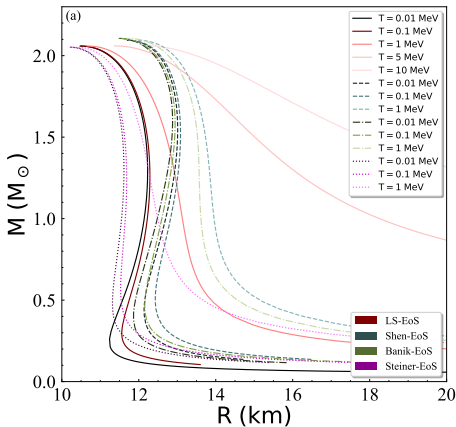
Last orbits of an inspiraling binary neutron star system

- Tidal heating effects are present during the inspiral → heating of the interior of neutron star
- Predictions for temperature: $T = 0.01 - 10 \text{ MeV}$
- To what extent the temperature, due to various mechanisms, affects the values of the tidal deformability of a neutron star during the inspiral process, just before the merger
- At temperatures $T = 0.01 - 10 \text{ MeV}$ the star's core is not particularly affected.
- Crust is much more sensitive to temperature. However, in the area of the mass size which is mainly detected by gravitational waves ($1.2\text{-}1.6 M_{\odot}$), the radius and consequently the tidal deformability, are particularly sensitive to the structure and size of the crust.

Last orbits of an inspiraling binary neutron star system

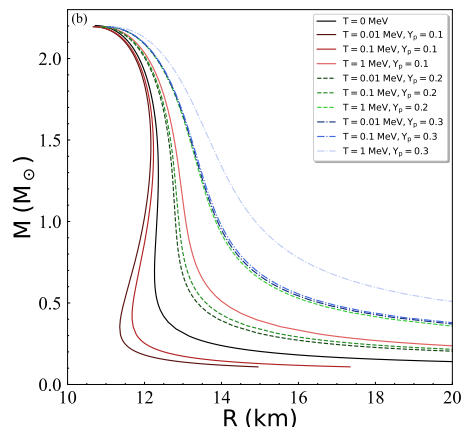
► Isothermal EOS: LS, Shen, Banik, Steiner

- $T = 0.01 - 1 \text{ MeV}$
- LS: $T = 10 \text{ MeV}$



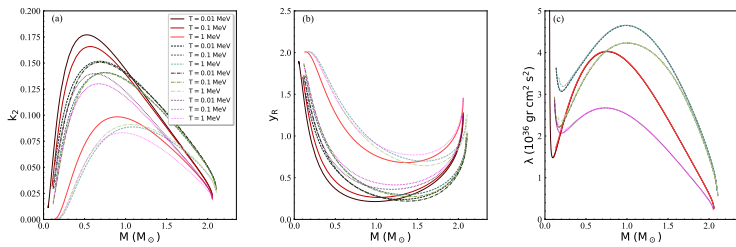
► Isothermal EOS: MDI+APR1

- $T = 0.01 - 1 \text{ MeV}$
- $Y_p = 0.1 - 0.3$



Love number - y_R - tidal deformability

- k_2 and y_R → strong sensitivity to the temperature
- λ → insensitive to the temperature (especially close to $M = 1.4 M_\odot$)



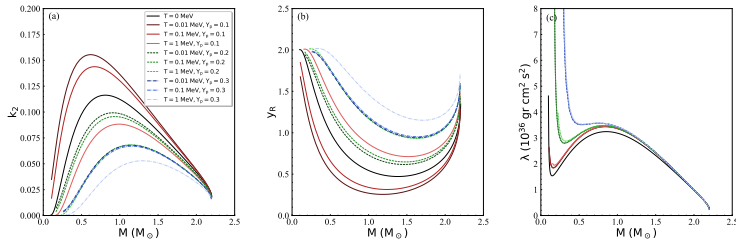
T (MeV)	k_2	R (km)	λ ($10^{36} \text{ gr cm}^2 \text{ s}^2$)
0.01	0.1005	12.21	2.73
0.1	0.0984	12.26	2.73
1	0.0788	12.82	2.73
5	0.0315	15.48	2.79
10	0.0127	18.92	3.02

$$\lambda = \frac{2}{3G} k_2 R^5$$

EOSs: LS, Shen, Banik, Steiner

Love number - y_R - tidal deformability

- k_2 and $y_R \rightarrow$ strong sensitivity to the temperature
- $\lambda \rightarrow$ insensitive to the temperature (especially close to $M = 1.4 M_\odot$)

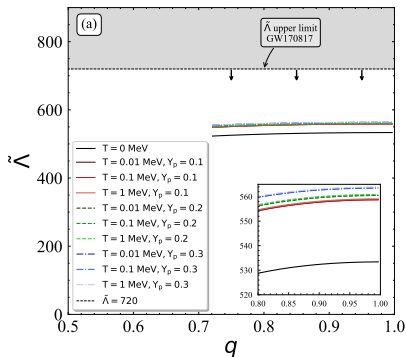


EOS: MDI+APR1

Effective tidal deformability

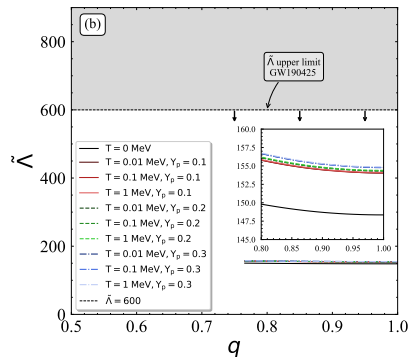
► GW170817

- $\mathcal{M}_c = 1.186 \text{ M}_\odot$



► GW190425

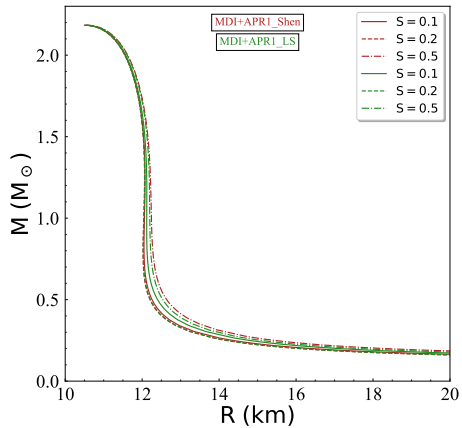
- $\mathcal{M}_c = 1.44 \text{ M}_\odot$



- Almost identical behavior for all the EOSs-families
- Thermal effects more pronounced in the GW170817 event → Binary neutron star mergers with a low value of chirp mass could be more suitable for this kind of study

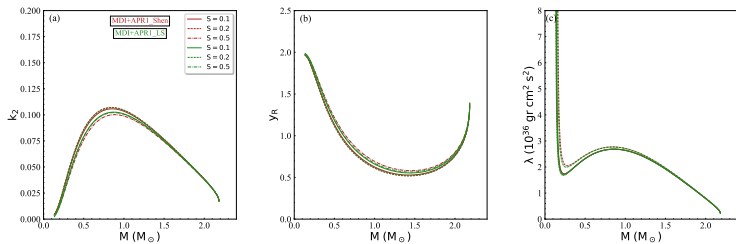
ISENTROPIC EOSs

- $S = 0.1 - 0.5 \text{ k}_B$
- $M_{\max} \rightarrow$ Temperature has insignificant effect
- $M_{1.4} \rightarrow$ Increasing temperature leads to increasing radius



Love number - y_R - tidal deformability

- Temperature has negligible effect on k_2 , $y_R \rightarrow \lambda$
- Similar predictions for each value of S

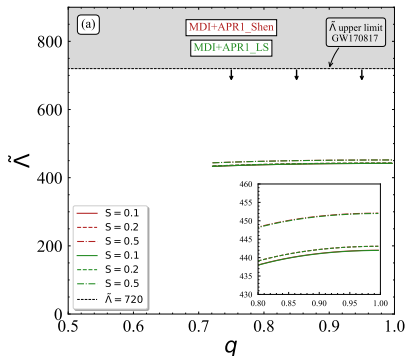


S (k_B)	Shen et al.			Lattimer and Swesty		
	k_2	R (km)	λ ($10^{36} \text{ gr cm}^2 \text{ s}^2$)	k_2	R (km)	λ ($10^{36} \text{ gr cm}^2 \text{ s}^2$)
0.1	0.0830	12.06	2.114	0.0817	12.10	2.114
0.2	0.0835	12.05	2.119	0.0834	12.05	2.119
0.5	0.0806	12.18	2.162	0.0814	12.16	2.161

Effective tidal deformability

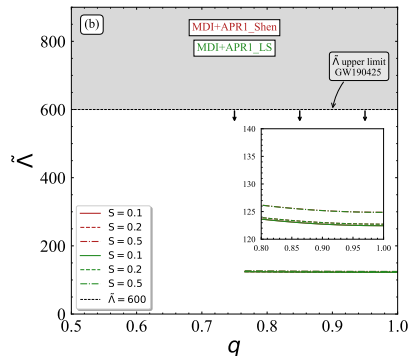
► GW170817

- $\mathcal{M}_c = 1.186 \text{ M}_\odot$



► GW190425

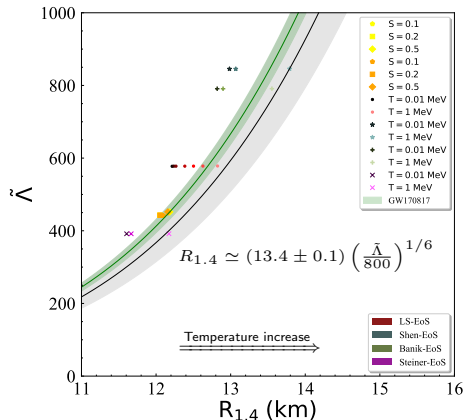
- $\mathcal{M}_c = 1.44 \text{ M}_\odot$



- Isentropic EOSs lead to lower values of $\tilde{\Lambda}$ than isothermal ones
- Binary neutron stars systems with higher value of chirp mass, such as the GW190425, minimize the differences between the EOSs

Effective tidal deformability and $R_{1.4}$

- GW170817
- Isentropic EOSs lie inside the boundaries
- Temperature increase → higher radii
- Possible constraints on the radius could lead to constraints on the value of the possibly existing temperature

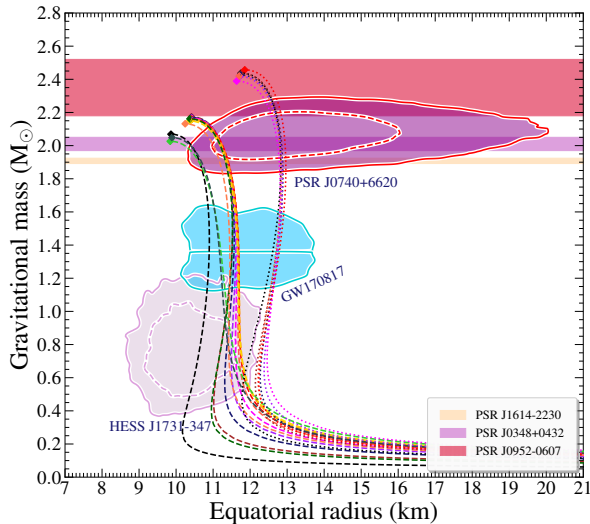


Microscopic properties of finite nuclei - GW events

- Relativistic nuclear energy density functionals → DD-PC and DD-ME ⁹
- Terrestrial experiments of nuclear physics: Parity violating electron scattering experiments → CREX and PREX-II
- Constrained microscopic quantities
 - weak form factors
 - neutron skin thickness
 - dipole polarizability
- Signal of GW → indicator of phase transition to exotic states of matter

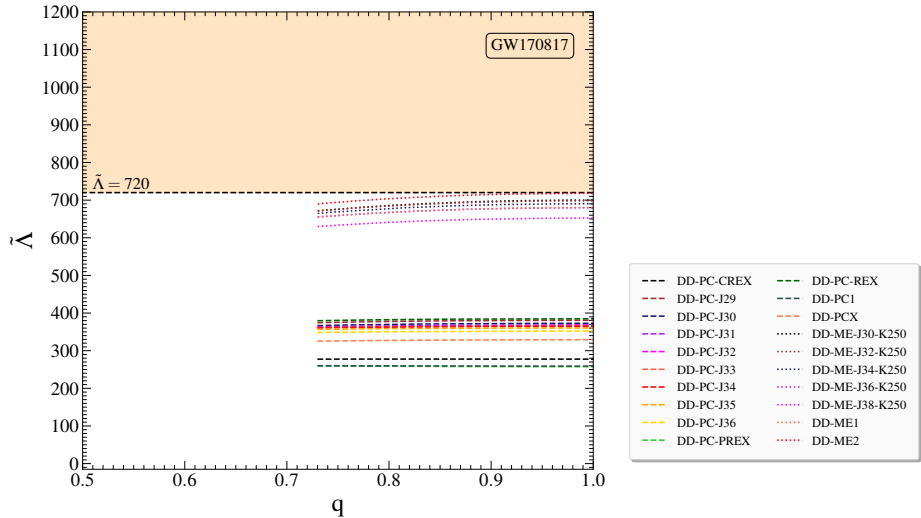
⁹ Esra Yüksel, Nils Paar, Phys. Lett. B **836**, 137622 (2023).

Mass-Radius relation



---	DD-PC-CREX	----	DD-PC-REX
- - -	DD-PC-J29	- - -	DD-PC1
- - -	DD-PC-J30	- - -	DD-PCX
- - -	DD-PC-J31	DD-ME-J30-K250
- - -	DD-PC-J32	DD-ME-J32-K250
- - -	DD-PC-J33	DD-ME-J34-K250
- - -	DD-PC-J34	DD-ME-J36-K250
- - -	DD-PC-J35	DD-ME-J38-K250
- - -	DD-PC-J36	DD-ME1
- - -	DD-PC-PREX	DD-ME2

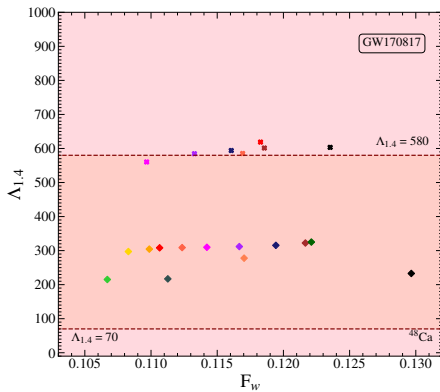
Effective tidal deformability



Weak form factor

► CREX: ^{48}Ca

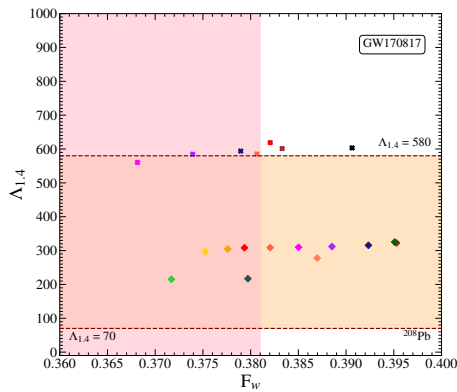
- $F_w = 0.1304 \pm 0.052 \pm 0.002$



◆ DD-PC-CREX	◆ DD-PC-J33	◆ DD-PC-REX	■ DD-ME-J34-K250
◆ DD-PC-J29	◆ DD-PC-J34	◆ DD-PC1	■ DD-ME-J36-K250
◆ DD-PC-J30	◆ DD-PC-J35	◆ DD-PCX	■ DD-ME-J38-K250
◆ DD-PC-J31	◆ DD-PC-J36	■ DD-ME-J30-K250	■ DD-ME1
◆ DD-PC-J32	◆ DD-PC-PREX	■ DD-ME-J32-K250	■ DD-ME2

► PREX-II: ^{208}Pb

- $F_w = 0.368 \pm 0.0132$

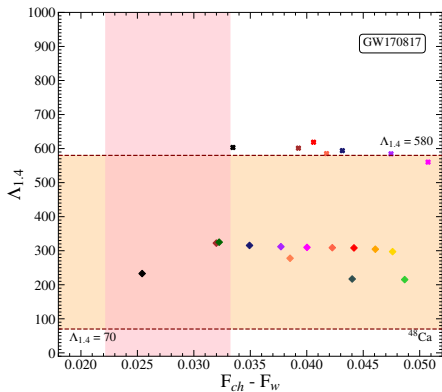


◆ DD-PC-CREX	◆ DD-PC-J33	◆ DD-PC-REX	■ DD-ME-J34-K250
◆ DD-PC-J29	◆ DD-PC-J34	◆ DD-PC1	■ DD-ME-J36-K250
◆ DD-PC-J30	◆ DD-PC-J35	◆ DD-PCX	■ DD-ME-J38-K250
◆ DD-PC-J31	◆ DD-PC-J36	■ DD-ME-J30-K250	■ DD-ME1
◆ DD-PC-J32	◆ DD-PC-PREX	■ DD-ME-J32-K250	■ DD-ME2

Charged form factor - Weak form factor

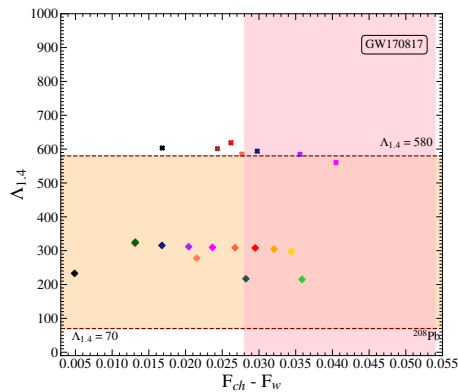
► CREX: ^{48}Ca

- $F_{ch} - F_w = 0.0277 \pm 0.0055$



► PREX-II: ^{208}Pb

- $F_{ch} - F_w = 0.041 \pm 0.013$



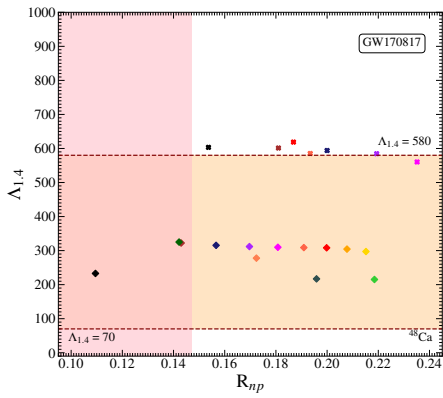
◆ DD-PC-CREX	◆ DD-PC-J33	◆ DD-PC-REX	■ DD-ME-J34-K250
◆ DD-PC-J29	◆ DD-PC-J34	◆ DD-ME-J36-K250	■ DD-PC1
◆ DD-PC-J30	◆ DD-PC-J35	◆ DD-ME-J38-K250	◆ DD-PC-J30
◆ DD-PC-J31	◆ DD-PC-J36	◆ DD-ME-J38-K250	◆ DD-PC-J31
◆ DD-PC-J32	◆ DD-PC-PREX	◆ DD-ME-J32-K250	◆ DD-PC-J32

◆ DD-PC-CREX	◆ DD-PC-J33	◆ DD-PC-REX	■ DD-ME-J34-K250
◆ DD-PC-J29	◆ DD-PC-J34	◆ DD-ME-J36-K250	■ DD-PC1
◆ DD-PC-J30	◆ DD-PC-J35	◆ DD-ME-J38-K250	◆ DD-PC-J30
◆ DD-PC-J31	◆ DD-PC-J36	◆ DD-ME-J38-K250	◆ DD-PC-J31
◆ DD-PC-J32	◆ DD-PC-PREX	◆ DD-ME-J32-K250	◆ DD-PC-J32

Neutron skin thickness

► CREX: ^{48}Ca

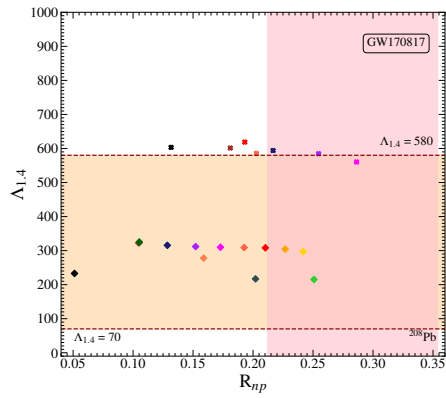
- $R_{np} = 0.121 \pm 0.026$ (fm)



◆ DD-PC-CREX	◆ DD-PC-J33	◆ DD-PC-REX	■ DD-ME-J34-K250
◆ DD-PC-J29	◆ DD-PC-J34	◆ DD-PC1	■ DD-ME-J36-K250
◆ DD-PC-J30	◆ DD-PC-J35	◆ DD-PCX	◆ DD-ME-J38-K250
◆ DD-PC-J31	◆ DD-PC-J36	◆ DD-ME-J30-K250	■ DD-ME-J30-K250
◆ DD-PC-J32	◆ DD-PC-PREX	■ DD-ME-J32-K250	■ DD-ME1
			■ DD-ME2

► PREX-II: ^{208}Pb

- $R_{np} = 0.283 \pm 0.071$ (fm)

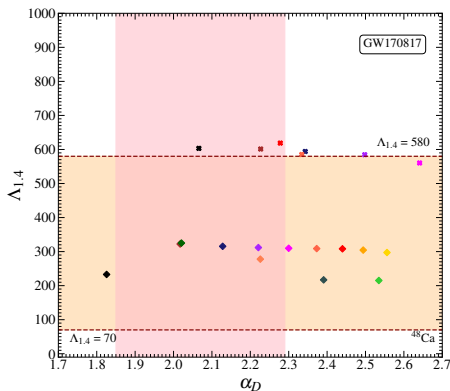


◆ DD-PC-CREX	◆ DD-PC-J33	◆ DD-PC-REX	■ DD-ME-J34-K250
◆ DD-PC-J29	◆ DD-PC-J34	◆ DD-PC1	■ DD-ME-J36-K250
◆ DD-PC-J30	◆ DD-PC-J35	◆ DD-PCX	◆ DD-ME-J38-K250
◆ DD-PC-J31	◆ DD-PC-J36	◆ DD-ME-J30-K250	■ DD-ME-J30-K250
◆ DD-PC-J32	◆ DD-PC-PREX	■ DD-ME-J32-K250	■ DD-ME1
			■ DD-ME2

Dipole polarizability

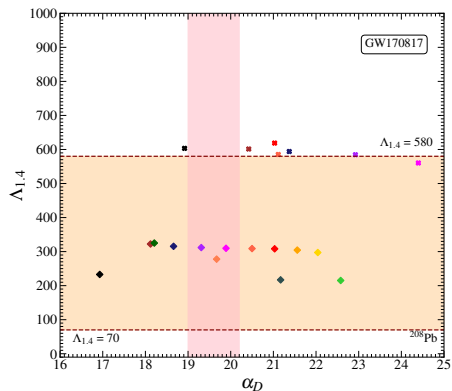
► ^{48}Ca

- $\alpha_D = 2.07 \pm 0.22 \text{ (fm}^3\text{)}$



► ^{208}Pb

- $\alpha_D = 19.6 \pm 0.6 \text{ (fm}^3\text{)}$



Concluding remarks

- As the entropy per baryon and temperature increases for isentropic EOSs, moment of inertia decreases leading to lower values of torques that the neutron star needs in order to change its rate of rotation than the cold case.
- The endpoint from Kerr parameter is that thermal support cannot lead a star to collapse into a maximally rotating Kerr black hole.
- As the temperature rises, instabilities driven by gravitational radiation would never occur in a hot, rapidly rotating neutron star.
- Temperature manifest significant effects on k_2 and y_R , but not on λ .
- The insensitivity of λ on the temperature applies regardless the EOS.
- Accurate measurements of the neutron star's radius can provide information about the temperature of the star before the merger.

Concluding remarks

- ▶ Preliminary results on the new constraints for the isolated neutron stars or binary neutron star system properties
 - In DD-PC EOSs the CREX favors low symmetry energy, while the PREX-II favors high values of symmetry energy.
 - CREX excludes the DD-ME EOSs, even the ones with low symmetry energy, while PREX-II requires high values of symmetry energy ($J = 38$ MeV).
 - In both cases, the dipole polarizability α_D favors low values of symmetry energy.
 - The results are in accordance with the CREX experiment
 - The results are not consistent to the PREX-II experiment for both DD-PC and DD-ME EOSs.

Thank you for your attention!

Collaborators

- Dr. N. Paar
- Dr. Ch. Moustakidis
- Dr. A. Kanakis-Pegios

Published papers

- P.S. Koliogiannis and Ch.C. Moustakidis, *Astrophys. J.* **912**, 69 (2021)
- A. Kanakis-Pegios, P.S. Koliogiannis, and Ch.C. Moustakidis, *Phys. Lett. B* **832**, 137267 (2022)

This work was supported by the Croatian Science Foundation under the project number HRZZ- MOBDOL-12-2023-6026 and by the Croatian Science Foundation under the project number IP-2022-10-7773.



Financira
Europska unija
NextGenerationEU



ARISTOTLE
UNIVERSITY
OF THESSALONIKI